Eur J Med Chem (1996) 31, 939–950

Photodynamic therapy of tumours: value of quantum chemical procedures for characterization of new drugs. Prediction of the electronic structure of zinc(II) phthalocyanine with special emphasis on triplet state excitation energies

M Ochsner*

Ciba-Geigy Ltd, Department of Physics, CH-4002 Basle, Switzerland

(Received 15 May 1996; accepted 13 June 1996)

Summary — Zinc(II) phthalocyanine is the active component of the liposomal formulation CGP 55847 which showed a high activity in photodynamic therapy in a variety of animal tumours. The photophysical properties of zinc(II) phthalocyanine have been studied in detail and compared to those of Photofrin, the only sensitizing agent approved so far for phase III/ IV clinical trials. Since the efficacy of photodynamic therapy intrinsically depends on the spectroscopic features of the sensitizer, quantum chemical methods have proven to be an efficient means for optimizing chemical structures. As will be shown, a simple modification of the time-honoured INDO model of Pople allows a prediction of the singlet and triplet state properties of molecules of the size of zinc(II) phthalocyanine with an rms error of ≤ 1000 cm^{-1}.

zinc(II) phthalocyanine / photodynamic therapy / INDO/S / quantum chemical prediction of spectral features / triplet state properties

Introduction

Photodynamic therapy

Photodynamic therapy (PDT) is an innovative and attractive modality for the treatment of small and superficial tumours. PDT, as a multi-modality treatment procedure, needs both a selective photosensitizer and a powerful light source that matches the absorption spectrum of the sensitizer. Quadra Logic's Photofrin, a purified haematoporphyrin derivative, is the only photosensitizer approved so far for phase III and IV clinical trials [1]. Major drawbacks of this product are lack of chemical homogeneity and stability, skin phototoxicity and unfavourable physicochemical properties [1]. The absorption spectrum of Photofrin possesses, as most porphyrins, an intense Soret band at around 400 nm and four weak transitions between 500 and 650 nm [2]. Unfortunately, the absorption coefficients ($\varepsilon_{630\ nm} \approx 3500$ M^{-1}·cm^{-1}) are very small in the red region of the spectrum, ie, at those wavelengths where the penetration depth of light reaches a maximum in most tissues [3]. Moreover, the low selectivity of Photofrin with regard to uptake and retention by tumour cells and the absorption of large fractions of sunlight may lead to strong skin phototoxic reactions [1, 2].

Second generation photosensitizers, including the phthalocyanines, show an increased photodynamic efficiency in the treatment of animal tumours and reduced phototoxic side effects [4–6]. At the time of the writing of this article, there were more than half a dozen new sensitizers in or about to start clinical trials. All available data suggest a common mechanism of action. Subsequent to excitation of the photosensitizer, the tumour is destroyed either by reactive singlet oxygen species (Type II mechanism) and/or radical products (Type I mechanism) generated in an energy transfer reaction.

In contrast to Photofrin, zinc(II) phthalocyanine is a pure and chemically well-defined lipophilic substance [1]. Since the photosensitizer absorbs at a longer wavelength ($\lambda_{max} \approx 670$ nm; $\varepsilon_{670\ nm} \approx 270\ 000$ M^{-1}· cm^{-1}; [1]), it is expected that zinc(II) phthalocyanine causes a deeper tumour necrosis than Photofrin [3]. In addition, the higher extinction coefficient (ε_S) of zinc(II) phthalocyanine lowers the drug dosage required to induce a cytotoxic response and the risk of provoking systemic toxic reactions is clearly diminished.

*Correspondence and reprints: Im Kugelfang, 40, CH-4102 Binningen, Switzerland.

A liposomal formulation of zinc(II) phthalocyanine for intravenous injection (CGP 55847) has been developed at Ciba Geigy Ltd and is currently undergoing phase I and II clinical trials at the CHUV (Centre hospitalier universitaire Vaudois de Lausanne, Switzerland) in patients suffering from squamous cell carcinomas of the upper aerodigestive tract [7, 8].

Type I and Type II reaction mechanisms

Upon absorption of light, sensitizer molecules are usually excited to a short-lived excited singlet state. Fast radiationless relaxation processes subsequently populate lower lying triplet states via intersystem crossing and ultimately yield the first excited triplet state T_1 in a spin-allowed process. The slower the decay of the triplet state, the more time the chemical has to act upon its environment, ie, the tumour tissue, via Type I or Type II reaction mechanisms and to initiate biochemical and biophysical mechanisms which cause the tumour necrosis [1, 2]. Since a long triplet state lifetime ($\tau_T > 1$ μs) is considered as a precondition for efficient photosensitization, molecules containing a diamagnetic central metal ion are consequently better suited for PDT than analogous compounds containing a paramagnetic metal ion, which drastically shortens the lifetime of the molecular triplet state [9, 10]. In addition, the effectiveness of the PDT treatment depends on various physiological and physicochemical properties and particularly on the number of photons absorbed by the photosensitizer per unit volume of tissue [1, 11]. A tumour necrosis can only occur if the number of absorbed photons exceeds a so-called damage threshold. For normal rat liver, sensitized by sulphonated chloroaluminium(III) phthalocyanine, the damage threshold was estimated to be 3.8 (±0.2) x 10^{19} photons/cm^3 [11].

If the energy of the first excited triplet state of a specific compound is lower than the excitation energy of $^1\Delta_gO_2$ (7900 cm^{-1}), the sensitizer molecules are generally not able to transfer their excitation energy to molecular oxygen ($^3\Sigma_g^-O_2$) and to generate $^1\Delta_gO_2$. The energy of the first excited triplet state of a photosensitizer should range between 7900 and 18 000 cm^{-1} to promote Type II mechanisms. Higher triplet state energies lead to unfavourable Franck–Condon factors which prevent an efficient coupling of the initial sensitizer–oxygen encounter complex to product states thereby inhibiting the generation of $^1\Delta_gO_2$ and/or highly excited $^1\Sigma_g^+O_2$ (excitation energy ≈ 13 200 cm^{-1}) [1, 12]. Notably, in condensed media, the lifetime of $^1\Sigma_g^+O_2$ is extremely short (τ_Σ = 20 ps in methanol [13]) and rapidly quenched to yield $^1\Delta_gO_2$ in a spin-allowed process [12].

However, there exist alternative pathways leading to the formation of $^1\Delta_gO_2$. An energy transfer from the S_1 state of the sensitizer to molecular oxygen with the subsequent generation of $^1\Delta_gO_2$ may occur, if the S_1–T_1 energy gap is greater than 7900 cm^{-1} and the sensitizer has a singlet state lifetime long enough ($\tau_S > 1$ μs) to allow ample bimolecular collisions with oxygen molecules [1, 12].

Compounds that have a triplet state energy below 7900 cm^{-1} but possess a high triplet state quantum yield and strong absorbance in the red or near infrared region (800–900 nm) may still be good candidates for Type I sensitizers if they possess long-lived excited singlet and/or triplet states (> 1 μs) with a high tendency of promoting electron-transfer reactions [1]. Since the competing reactions leading to the formation of $^1\Delta_gO_2$ are energetically inhibited, radicals from endogenous substrates (amino acids and/or alcohols) may be generated with high efficiency [1].

Methods

Prediction of spectroscopic features using a Hartree–Fock–SCF formalism

For large molecular systems, the most rewarding approach to determine the energy of the electronic ground state has been to linearly expand the molecular orbitals in terms of a limited set of atomic eigenfunctions, to define a proper Hartree–Fock operator, calculate the energy of the electronic ground state, apply the variation principle, set up the Roothaan equations and solve them. Based on the variation method, the best choice of molecular orbitals for the ground state configuration is obtained by varying the coefficients of the contributing atomic wavefunctions in the determinant until the energy achieves its minimum. These orbitals are referred to as self-consistent field Hartree–Fock molecular orbitals (SCF MOs). To obtain reasonable estimates of the excitation energies of the lowest lying singlet and triplet states, these SCF MOs enter a configuration interaction (CI) calculation yielding the desired spectroscopic transition frequencies and oscillator strengths.

Considerable success has been met in organizing the $\pi \rightarrow \pi^*$ spectra of aromatic molecules by using the Pariser–Parr–Pople SCF CI model [14]. Extensions of this method, still within the π-electron framework, incorporated lone pairs and inductive effects and allowed a rudimentary assignment of $n \rightarrow \pi^*$ transitions [15].

Toward the goal of predicting the effect of lone pair electrons on the electronic spectra of unsaturated molecules, Del Bene and Jaffé reparameterized Pople's CNDO/2 model [16, 17] and reproduced many of the spectral features of nitrogen and carbonyl containing compounds, although with low accuracy [18, 19].

Stimulated by these results, Ridley and Zerner revised Pople's INDO/1 model [17, 20] and calculated the singlet and triplet absorption spectra of a wide variety of heterocyclic molecules with an rms error of less than 1000 cm^{-1} [21, 22]. Notably, the INDO method possesses the distinct advantage over the CNDO model that upon inclusion of one-center, two-electron exchange integrals, $\sigma \rightarrow \pi^*$ and $\pi \rightarrow \sigma^*$ transitions of different multiplicities are split in energy as, indeed, they should be.

To accurately predict the manifold of singlet and triplet states for molecules of the size of zinc(II) phthalocyanine, the reliability of various semiempirical programs (Extended Hückel, CNDO/S, INDO/S, MINDO/3, MNDO, MOPAC and PPP) with numerous parameterizations has been studied. In conclusion we have given preference to the INDO/S model of Zerner.

The INDO/S model

The molecular ground state and its energy

Theoretical considerations. In order to solve the time-independent Schrödinger equation for a specific molecular system ($\mathbf{H}_{el} \cdot \Psi_{el} = E_{el} \cdot \Psi_{el}$) and obtain reasonable estimates of the ground state wavefunction (Ψ_{GS}) and energy (E_{GS}), the molecular wavefunction (Ψ_{GS}) is approximated by an antisymmetrized and normalized product of molecular spin orbitals. For a system containing q β electrons and p ($> q$) α electrons, the Hartree–Fock determinant is represented by:

$$^{p-q+1}\Psi_{GS} = |(p+q)!|^{-1/2} \, | \, \phi_1^{\alpha}(1) \, \alpha(1) \, \phi_1^{\beta}(2) \, \beta(2) \ldots \phi_q^{\alpha}(2q-1) \, \alpha(2q-1) \, \phi_q^{\beta}(2q) \, \beta(2q) \ldots \phi_p^{\alpha}(p+q) \, \alpha(p+q) |$$

where the product of spatial orbital and spin functions is designated as molecular spin orbital χ_i ($i = 1, \ldots, [p+q]$); for example $\chi_{2q} = \phi_q^{\beta}(2q) \, \beta(2q)$.

Based on the Roothaan–Hall recipe [23, 24], the molecular wavefunctions (ϕ_i^k) are expanded as linear combination of all-valence atomic orbitals (θ_μ):

$$\text{LCAO} - \text{MO}: \; \phi_i^k = \sum_{\mu=1}^{M} C_{\mu i}^k \cdot \theta_\mu$$

where the superscript k either denotes α or β spin for the closed-shell spin-restricted ($\phi_i^{\alpha} = \phi_i^{\beta}$) [21] or spin-unrestricted case [25–27] or most often refers to a shell structure for an open-shell, spin-restricted calculation [28]. Within the frame of Zerner's INDO/S method, the atomic orbitals (AOs) of first, second and third row elements are represented by ordinary Slater-type orbitals (STOs). Except for the 1s AO on the hydrogen atom ($\zeta = 1.2$), all orbital exponents (ζ) were obtained from Slater's rule [29]. For fourth and fifth row elements double-ζ basis functions [30] have been chosen to match the moments of relativistic atomic Hartree–Fock calculations. In addition, a lot of emphasis was put on the structure of d-orbital functions, since regular d-STOs concentrate too much electron density in the bonding region [25, 26]. Recently, the INDO/S model has been extended to the f-electron lanthanide series [31]. However, since the prediction of the spectral features of lanthanide-containing compounds requires the inclusion of additional terms in the Hamiltonian to account for spin-orbit coupling effects [31], we shall not further discuss the spectroscopic properties of organometallic lanthanides in this context.

Application of the variation principle yields the Roothaan equations which reduce to the standard eigenvalue problem by adopting Pople's zero differential overlap (ZDO) approximation [17, 21]:

$$\mathbf{F}^k \cdot \mathbf{C}_i^k = \varepsilon_i^k \cdot \mathbf{C}_i^k$$

Here $\mathbf{F}^k$ represents the Fock or energy matrix, the column vector $\mathbf{C}_i^k$ contains the coefficients $C_{\mu i}^k$ of molecular orbital ϕ_i^k and ε_i^k specifies its energy. Since the basis functions are envisioned to be strongly orthonormal (ZDO approximation), disregarding the fact that non-orthogonal Slater-type orbitals are used throughout the calculation, the semiempirical parameters in the Fock matrix (see below) need to be adjusted to compensate for the inconsistencies introduced.

Within the scheme of Zerner's INDO/S model, the matrix elements $F_{\mu\nu}^k$ of the molecular ground state are specified by [25–27]:

$$F_{\mu\mu}^k = U_{\mu\mu} + \sum_{\sigma,\lambda}^{A} [P_{\sigma\lambda}\langle\mu\mu|\sigma\lambda\rangle - P_{\sigma\lambda}^k\langle\mu\sigma|\mu\lambda\rangle] + \sum_{B \neq A} \left[\sum_{\sigma}^{B} [(P_{\sigma\sigma} - 1) \cdot \gamma_{\mu\sigma}^{AB}] \right]; \; \mu \in A$$

$$F_{\mu\nu}^k = \sum_{\sigma,\lambda}^{A} [P_{\sigma\lambda}\langle\mu\nu|\sigma\lambda\rangle - P_{\sigma\lambda}^k\langle\mu\sigma|\nu\lambda\rangle]; \; \mu, \nu \in A$$

$$F_{\mu\nu}^k = \overline{S}_{\mu\nu} \cdot [\beta_{A,\mu} + \beta_{B,\nu}]/2 - P_{\mu\nu}^k \cdot \gamma_{\mu\nu}^{AB}; \; \mu \in A; \nu \in B$$

Specification of the parameters. The one-center core integral, $U_{\mu\mu}$, is calculated from a 'weighted' atomic ionization potential (I_μ) and thus incorporates the effects of a core pseudo-potential $V_{\mu\mu}$ which simulates the repulsion of inner shell electrons [25–27].

Z_A represents the nuclear core charge of atom A and $\beta_{A,\mu}$ is an empirical bonding parameter chosen to give

best agreement with experimental data. Each atom has at most two parameters $\beta_{A,\mu}$, where the same parameter is used for s and p atomic orbitals, $\beta_{A,s} = \beta_{A,p}$, but a different value is chosen for atomic d orbitals $\beta_{A,d}$ [26, 27].

The first-order Fock–Dirac density matrix ($\mathbf{P} = \mathbf{P}^{\alpha} + \mathbf{P}^{\beta}$) is defined by:

$$P^{\alpha}_{\mu\nu} = \sum_{i=1}^{p} C^{*\alpha}_{\mu i}\, C^{\alpha}_{\nu i};\; P^{\beta}_{\mu\nu} = \sum_{j=1}^{q} C^{*\beta}_{\mu j} \cdot C^{\beta}_{\nu j}$$

with the summation taken over all α (or β) spin MOs occupied in the molecular ground state.

The one-center, two-electron integrals, $\langle\mu\nu|\sigma\lambda\rangle$ are calculated from [26]:

$$\langle\mu\nu|\sigma\lambda\rangle = \int\int \frac{\theta^{*}_{\mu}(1)\theta_{\nu}(1) \cdot \theta^{*}_{\sigma}(2)\theta_{\lambda}(2)}{r_{12}} dv_1 \cdot dv_2;$$

$$\mu, \nu, \sigma, \lambda \in \mathrm{A}$$

Within the frame of Pople's standard INDO procedure only those corrections are preserved which correspond to the exchange $\langle\mu\nu|\mu\nu\rangle$ and Coulomb $\langle\mu\mu|\nu\nu\rangle$ integrals, respectively [17]. However, Zerner retains all those integrals that include Slater–Condon F, G and R integrals, such as the hybrid type integral $\langle p_x d_{yz}|p_z d_{xy}\rangle$, to preserve rotational invariance for atoms containing s, p and d atomic basis functions [27, 32].

The two-center, two-electron Coulomb integrals, $\gamma^{AB}_{\mu\nu}$, are approximated by semiempirical expressions adopting a different parameterization for calculation of singlet and triplet state energies (see below) and the weighted two-center overlap integrals, $\overline{S}_{\mu\nu}$, are related to the ordinary orbital overlap integrals, $S_{\mu\nu}$, of Pople by [17, 25, 26]:

$$\overline{S}_{\mu\nu} = \sum_{u} g_{\nu(u)} \cdot f_{\nu(u)} \cdot S_{\mu(u)\nu(u)}$$

Based on the mathematical structure of the orbital functions and their relative positions, the proper overlap matrix is immediately obtained. The Eulerian transformation matrices ($g_{p\sigma}$, $g_{p\pi}$, $g_{d\sigma}$, $g_{d\pi}$, $g_{d\delta}$, ...) are required to rotate the local diatomic to the molecular coordinate system and the f-terms ($f_{p\sigma}$, $f_{p\pi}$, $f_{d\sigma}$, $f_{d\pi}$, $f_{d\delta}$, ...) are universal weighting factors which describe an admixing of σ-, π- or δ-properties to overlap integrals $\overline{S}_{\mu\nu}$ of the type $\overline{S}_{pp}$ and $\overline{S}_{dd}$ [25, 26].

The geometry of the system is clearly reflected in the overlap matrix. If experimental data are not available, an idealized geometry (regular polygons, bond length and bond angles) may be used throughout the calculation. For larger molecules it is, however, recommended to optimize the structure with a dedicated software package prior to calculating the molecular spectrum. Starting with an initial geometry, the molecular energy is minimized in terms of its structure either by quantum chemical or by molecular mechanical procedures. The major distinction between the two methods is that in the molecular mechanics approach the electrons are not considered explicitly and the various atoms are treated as units interconnected by specific potentials [33, 34]. The potential functions depend on van der Waals radii, bond lengths, bond angles, stretching and bending force constants, etc [33]. In Allinger's MM2 program, the force field has been parameterized to yield excellent geometries, relative conformational energies, heats of formation, crystal packing arrangements and reactivities [34]. However, the geometries obtained using Zerner's non-spectroscopic INDO/1 version [25, 35] or Stewart's MOPAC program [36], a semiempirical all-valence-electron calculation (utilizing the AM1 Hamiltonian), are generally better suited for subsequently predicting spectral transitions. Starting at an arbitrary geometry and guided by an iterative Newton or Hessian procedure, one steps to the energy minimum ($E_{tot} = E_{el} + E_{nuc}$; see below) until all gradients (first and second derivatives of the total energy) are equal to zero [37]. In our experience, the INDO/1 structures seem to be superior to the MOPAC geometries at least for phthalocyanine and porphyrin ring systems, because they result in totally planar π-systems. Apparently, the AM1 Hamiltonian tends to attribute to much single bond character to the bonds between the isoindole rings and aza nitrogen atoms, so that a torsion around these bonds may occur.

Calculation of the molecular ground state using the INDO/S method. Based on initial estimates of the density matrices $P^{k}_{\mu\nu}$, an SCF calculation is performed and the ground state configuration calculated. The starting set of MO coefficients is generated by diagonalizing a Hückel-like matrix constructed from:

$$F^{0,k}_{\mu\mu} = -I_{\mu}/2$$

$$F^{0,k}_{\mu\nu} = \overline{S}_{\mu\nu} \cdot (\beta_{A,\mu} + \beta_{B,\nu})/2;\; \mu \neq \nu$$

By inserting the eigenvalues (ε^{k}_{i}) thus obtained into the Roothaan equations ($\mathbf{F}^{0,k} \cdot \mathbf{C}^{k}_{i} = \varepsilon^{k}_{i} \cdot \mathbf{C}^{k}_{i}$), a refined set of coefficient matrices $\mathbf{C}^{k}_{i}$ is gained and yields initial estimates of the first-order density matrices $P^{k}_{\mu\nu}$ and of the electronic energy of the molecular ground state:

$$E_{el} = 1/2 \sum_{i}^{p} \left[2 \cdot \varepsilon^{\alpha}_{i} - \sum_{j}^{p} [J^{\alpha\alpha}_{ij} - K^{\alpha\alpha}_{ij}] - \sum_{j}^{q} J^{\alpha\beta}_{ij} \right]$$

$$+ 1/2 \sum_{i}^{q} \left[2 \cdot \varepsilon^{\beta}_{i} - \sum_{j}^{q} [J^{\beta\beta}_{ij} - K^{\beta\beta}_{ij}] - \sum_{j}^{p} J^{\beta\alpha}_{ij} \right]$$

which when added to the energy accounting for the internuclear repulsion, E_{nuc}, provides an expression for the total energy:

$$E_{tot} = E_{el} + E_{nuc}$$

$$E_{nuc} = \sum_{A \neq B} Z_A \cdot Z_B / R_{AB}$$

Here R_{AB} corresponds to the distance between the two centers (A, B), while J_{ij} and K_{ij} are identified with the Coulomb and exchange integrals, respectively:

$$J_{ij}^{\alpha\beta} = \int\int \frac{\phi_i^{*\alpha}(1)\phi_i^{\alpha}(1) \cdot \phi_j^{*\beta}(2)\phi_j^{\beta}(2)}{r_{12}} dv_1 \cdot dv_2$$

$$K_{ij}^{\alpha\alpha} = \int\int \frac{\phi_i^{*\alpha}(1)\phi_j^{\alpha}(1) \cdot \phi_j^{*\alpha}(2)\phi_i^{\alpha}(2)}{r_{12}} dv_1 \cdot dv_2$$

The Coulomb repulsion integral, $J_{ij}^{\alpha\beta}$, represents the interaction of the smoothed-out charge distributions $\phi_i^{*\alpha} \cdot \phi_i^{\alpha}$ and $\phi_j^{*\beta} \cdot \phi_j^{\beta}$. The exchange integral, $K_{ij}^{\alpha\alpha}$, is a typical quantum mechanical quantity without any classical analogue. $K_{ij}^{\alpha\alpha}$ enters the two-electron coupling term with a negative sign and reduces the energy of interaction between electrons with parallel spins in different orbitals ϕ_i^{α} and ϕ_j^{α}. Upon using the symmetry properties of the molecule under consideration, the number of two-electron integrals reduces to those being unique by symmetry. Detailed directions for the calculation of Coulomb and exchange integrals within the INDO/S approximation are found in reference [21].

The elements of the first-order density matrices $P_{\mu\nu}^k$ are ultimately used to construct new Hartree–Fock matrices $\mathbf{F}^k$. The simultaneous diagonalization of these matrices, which are linked through the first-order density matrix $P_{\mu\nu}$, leads to an improved set of expansion coefficients $C_{\mu i}^k$ and the iterative process is repeated until self-consistency is achieved, ie, until:

$$[E_{el}^{(n)} - E_{el}^{(n-1)}] < 10^{-7} \text{ Hartree}$$

where $E_{el}^{(n)}$ gives the electronic energy after n iterations.

The full configuration interaction (CI) matrix

The most rewarding approach to obtain reliable estimates of the manifold of molecular states consists of setting-up and diagonalizing the full configuration interaction matrix [30]. The corresponding determinantal wavefunctions Ψ_s ($s > 0$) are constructed by replacing one or more of the occupied molecular spin orbitals χ_i in the ground state Slater determinant by virtual spin orbitals. The excited configurations are classified into single-substitution functions, $\Psi_{i \to a}$, in which a single electron is promoted from a filled χ_i to a virtual spin orbital χ_a, double-substitution functions, $\Psi_{ij \to ab}$, in which χ_i is replaced by χ_a and χ_j by χ_b, triple-substitution functions, $\Psi_{ijk \to abc}$, and so forth. Within the framework of the full CI method the exact determinantal wavefunctions, Ψ_i, are obtained by solving the proper secular equation [30]:

$$\Psi_i = a_{0i} \cdot \Psi_0 + \sum_{s>0} a_{si} \cdot \Psi_s \text{ with } \langle \Psi_s | \Psi_t \rangle = \delta_{st}$$

$$\sum_s (H_{st} - E_i \cdot \delta_{st}) a_{si} = 0\,;\; t = 0, 1, 2, \cdots$$

where the CI matrix elements H_{st} are defined by:

$$H_{st} = \langle \Psi_s | \mathbf{H} | \Psi_t \rangle$$

The full CI method is well defined, size-consistent and variational. However, due to the large number of substituted determinantal wavefunctions, the procedure is very time-consuming and limited to small molecular systems [30].

The CI matrix within the INDO/S framework

Zerner's INDO/S model has been finely tuned to reproduce the spectral features of a wide variety of heterocyclic compounds by considering single excitations only. The truncation of the full CI matrix by restriction on single-substitution functions is termed as a limited configuration interaction treatment. As we are mainly interested in predicting the spectroscopic features of large molecular systems, we focus our treatment (without a considerable loss in generality) on molecules whose ground state possesses a closed-shell structure. Excitation of an electron from a filled χ_i to a virtual spin orbital χ_a consequently gives rise to singlet and triplet state configurations. Because the spin functions between electron configurations of different multiplicity are mutually orthogonal, $\langle {}^1\Psi_{i \to a} | \mathbf{H} | {}^3\Psi_{j \to b} \rangle = 0$, the CI matrix partitions into two independent blocks.

By considering only single excitations in the CI matrix, no improvement of the ground state determinant is possible, since the matrix elements which couple the molecular ground state to singly excited configurations vanish (Brillouin's theorem). That means, if the MOs are completely self-consistent, the ground state determinant is, by definition, the best single determinantal wavefunction and cannot be improved by a configuration interaction treatment. However, within the limitations imposed by the SCF MO basis set, excited state wavefunctions are not adequately described as single Slater determinants, ie, the single-substitution functions ${}^{1(3)}\Psi_{i \to a}$ generated by promoting an electron from an occupied (χ_i) to an

unoccupied (χ_a) spin orbital are not eigenfunctions of the CI Hamiltonian **H**. Since most off-diagonal matrix elements accounting for interactions between singly excited electron configurations are non-zero (see below), diagonalization of the CI matrix is required to get the desired transition energies and to determine the structure of excited state wavefunctions which are ultimately expressed as linear combination of single-substitution determinants. To obtain reasonable estimates of the lowest lying singlet and triplet states, the number of single-substitution functions which need to be included in the CI matrix drastically increases with the size of the molecule. Moreover, because the CI matrix only considers single excitations and neglects interactions with and between multi-substitution wavefunctions, the set of semiempirical parameters unquestionably contains contributions which compensate for the truncation of the CI matrix. Anyway, no such parameterization can neutralize multiple excited configurations if the corresponding transitions lie in the spectroscopic region of interest, or if double-substitution determinants heavily mix with the ground state configuration. Within the frame of the INDO/S model higher substitution wavefunctions may be quite easily incorporated in the CI matrix [30, 38, 39]. However, care is advised. Since the parameterization has been calibrated at the CI-singles level, the inclusion of double-substitution wavefunctions often leads to an overestimation of the transition frequencies by drastically lowering the ground state energy. The balance is generally not restored until certain triply excited configurations are included in the CI matrix.

The singlet state CI matrix within the INDO/S framework. The zero-order excitation energy associated with a singlet-singlet transition is computed from:

$$\Delta E_{ia}^{kk} = \varepsilon_a^k - \varepsilon_i^k - J_{ia}^{kk} + 2 \cdot K_{ia}^{kk}$$

where the quantities, J_{ia}^{kk} and K_{ia}^{kk}, correspond to the Coulomb and exchange integrals, respectively.

The manifold of these transition energies enter the CI matrix as diagonal elements, $\langle {}^1\Psi_{i\to a}^{kk}|\mathbf{H}|\,{}^1\Psi_{i\to a}^{kk}\rangle$ where the superscript kk denotes excitation within the subspace of α or β spin MOs. The off-diagonal CI matrix elements are identified with [21]:

$$\langle\, {}^1\Psi_{GS}|\mathbf{H}|\,{}^1\Psi_{i\to a}^{kk}\rangle = 0 \qquad \text{(Brillouin's theorem}$$

$$\langle\, {}^1\Psi_{i\to a}^{kk}|\mathbf{H}|\,{}^1\Psi_{j\to b}^{k'k'}\rangle = 2\cdot\langle ai|jb\rangle - \langle ab|ij\rangle$$

Detailed directions for the calculation of the integrals $\langle ai\,|\,jb\rangle$ and $\langle ab\,|\,ij\rangle$ are found in the appendix of reference [21] where a proper consideration of the orthogonality of the molecular spin orbitals is implied. Note that $\langle ab|ij\rangle$ vanishes unless $k = k'$.

The triplet state CI matrix within the INDO/S framework. With reference to the electronic ground state, the zero-order singlet-triplet transition energies are given by:

$$\Delta E_{ia}^{kk'} = \varepsilon_a^{k'} - \varepsilon_i^k - J_{ia}^{kk'} \text{ with } k \neq k'$$

and enter the triplet state CI matrix as diagonal elements, $\langle {}^3\Psi_{i\to a}^{kk'}|\mathbf{H}|\,{}^3\Psi_{i\to a}^{kk'}\rangle$. Notably, excitation of the molecular ground state to an excited triplet state is associated with a spin-flip reaction and a change in the spin angular momentum.

The off-diagonal matrix elements of the triplet CI matrix are calculated from:

$$\langle\, {}^1\Psi_{GS}|\mathbf{H}|\,{}^3\Psi_{i\to a}^{kk'}\rangle = 0 \qquad \text{(Spin orthogonality)}$$

$$\langle\, {}^3\Psi_{i\to a}^{kk'}|\mathbf{H}|\,{}^3\Psi_{j\to b}^{kk'}\rangle = -\langle ab|ij\rangle \quad \text{with } k \neq k'$$

The parameterization scheme within the INDO/S model

Since electronic excitations occur without change of nuclear geometry (Franck–Condon principle), the semiempirical parameters have been calibrated to the band maxima of well-known spectroscopic transitions. This seems most reasonable as we are estimating a point on the potential surface of the ground state near its experimental minimum and points on the potential surfaces of excited states directly above the ground state minimum ('vertical transition').

Towards the goal of incorporating the effects of higher excitations within the framework of the limited CI method, it was, however, unavoidable to choose a different parameterization for reproducing the manifold of singlet and triplet state energies.

The singlet state parameterization. The semiempirical parameters $\beta_{A,\mu}$, the f-values ($f_{p\sigma}$, $f_{p\pi}$,...) and the two-center, two-electron Coulomb integrals, $\gamma_{\mu\nu}^{AB}$, were fitted to minimize the ground state energy and to reproduce the spectral features of a wide variety of molecular systems (benzene, pyridine, pyrrole, etc). After an extensive search, the Coulomb integral, $\gamma_{\mu\nu}^{AB}$, was approximated using the Weiss modification of the Mataga–Nishimoto recipe [40]:

$$\gamma_{\mu\nu}^{AB} = \frac{f_\gamma}{2\cdot f_\gamma[\gamma_{\mu\mu}^{A} + \gamma_{\nu\nu}^{B}]^{-1} + R_{AB}}$$

where R_{AB} corresponds to the distance between the two centers (A, B) and $\gamma_{\mu\mu}^{A}$ to the difference between

the ionization potential (I_μ^A) and electron affinity (A_μ^A) of an s, p or d electron of atom A, ie, $\gamma_{\mu\mu}^A = I_\mu^A - A_\mu^A$ [27, 41]. Following the recommendation of Weiss (unpublished results, 1970), the parameter f_γ was set to 1.2 to raise the value of the Coulomb integral above that of the unmodified Mataga–Nishimoto equation [40].

The triplet state parameterization. It is, perhaps, not surprising that a model which is finely tuned to estimate singlet-singlet transition frequencies is far less successful in predicting triplet state energies. This is especially true because the configuration matrix includes only singly excited configurations. The omission of multi-substitution wavefunctions strongly affects the values of the semiempirical parameters ($\beta_{A,\mu}$, $\gamma_{\mu\nu}^{AB}$ and $f_{p\sigma}$, $f_{p\pi}$, $f_{d\delta}$,...) which were carefully adjusted to accurately predict the singlet-singlet transition frequencies of a wide variety of molecular species. A different parameterization was therefore adopted for the calculation of triplet-triplet absorption spectra.

After investigating the various empirical approximations used in the INDO/S method, Zerner concluded that the two-center Coulomb integral, $\gamma_{\mu\nu}^{AB}$, needs to be modified to improve the prediction of triplet state energies. The physical justification for this adjustment relies on the fact that the correlation between two electrons with parallel spin is smaller than that between electrons with antiparallel spin [41]:

For $R_{AB} < 280$ pm

$$\gamma_{\mu\nu}^{AB} = (\gamma_{\mu\mu}^{A} + \gamma_{\nu\nu}^{B})/2 - a \cdot R_{AB} - b \cdot R_{AB}^2$$

For $R_{AB} \geq 280$ pm

$$\gamma_{\mu\nu}^{AB} = ([1 + [(r_A - r_B)/(2 \cdot R_{AB})]^2]^{-1/2} + [1 + [(r_A + r_B)/(2 \cdot R_{AB})]^2]^{-1/2})/(2 \cdot R_{AB})$$

where r_A is inverse proportional to the effective nuclear charge Z_A ($r_A = 8.687/Z_A$). Least-square values for the parameters a and b are found in reference [22].

To further improve the predictive power of the INDO/S model to estimate triplet-triplet absorption spectra, Ridley and Zerner advise to change the overlap integral weighting factor $f_{p\pi}$ to 0.68 [22]. However, based on an extensive least-squares search, a value of $f_{p\pi} = 0.72$ yields better estimates of triplet-triplet transition frequencies at least for porphyrin and phthalocyanine ring systems (M Ochsner, unpublished results, 1992). In our experience, it is generally recommended to determine the best fitting value for a distinct class of ring systems. The parameter $f_{p\pi}$ should, however, lie in the range between 0.64 and 0.74 to not overstress the model. If not specified otherwise, the default value of 0.68 is selected.

A summary of Zerner's singlet and triplet parameterization scheme is found in references [22, 25, 27].

Results and discussion

The molecular structure of zinc(II) phthalocyanine

The ring system of zinc(II) phthalocyanine (ZnPc) is displayed in figure 1 and basically consists of four isoindole rings linked by aza bridges with a positively charged zinc(II) atom at the symmetry center [42].

As expected on the basis of the simple Hückel theorem, the ground state of ZnPc is planar and has a symmetry of D_{4h}. X-ray diffraction data only reveal slight deviations from D_{4h} symmetry indicating that the dihedral angle between the pyrrole and its associated benzene ring is less than 1.2° [43]. In agreement with the Hückel model all thermal parameters of the zinc(II) atom (tables II and V in reference [43]) are only consistent with a zinc(II) atom positioned at the symmetry center. The average Zn-N bond length is unusually short (198.0 (±0.2) pm) as compared to other zinc complexes (see below).

Recently, the molecular structure of ZnPc has been determined in the gas phase using the electron diffraction technique [44]. As discussed in detail by Burkert and Allinger, the geometries derived from the X-ray or electron diffraction method may be quite different [45]. The tight packing of the molecules in the crystal leads to a force field which might cause slight distortions of the equilibrium geometry. In addition, differ-

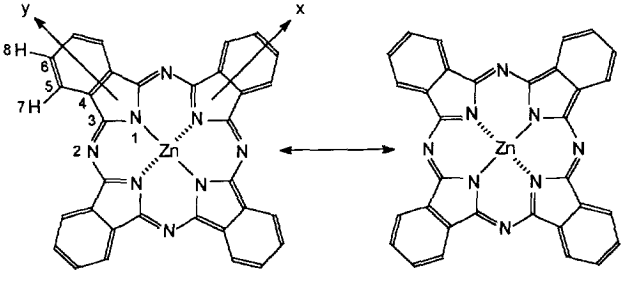

Fig 1. The zinc(II) phthalocyanine molecule consists of four isoindole rings linked by aza bridges with a zinc(II) atom at the symmetry center. Owing to the high symmetry of the macrocycle (D_{4h}), there are two unique choices for the orientation of the x- and y- axes; ie, either the aza or pyrrole nitrogens may be chosen to define these axes. We decided to align the axes along the pyrrole nitrogens, since the Jahn–Teller effect couples the degenerate wavefunctions of the first excited singlet state $|^1E_u^Q(\pi^*)\rangle$ to b_{1g} vibrational modes (see fig 2) thereby distorting the molecular frame to configurations which transform like the x- and y-coordinates.

ences occur, because X-rays 'see' (are scattered by) electron clouds, while electrons are scattered by nuclei [45]. For atoms other than hydrogen, these differences are small. Since the bonding electrons are the only electrons around the hydrogen nucleus, those bond lengths involving hydrogen atoms are persistently too short when measured by X-ray crystallography. A deficiency of electron diffraction technique is the fact that a reduction of the molecular symmetry from D_{4h} to D_{2h} cannot be observed, since the diffraction pattern is generated by a large number of randomly oriented molecules and yields a structure which is averaged over singular distortions [45]. Due to the regular arrangement of ZnPc molecules in the crystal (space group $P2_1/a$; $Z = 2$), such distortions could principally be detected in the X-ray structure. Despite qualitative differences between the two methods, the geometry of ZnPc derived from the electron diffraction technique closely matches the X-ray structure indicating that crystal-packing forces lead to a negligible distortion of the molecular frame. Contrasting these results, the electron diffraction pattern is only consistent with a zinc(II) atom found out of the plane of the molecule reducing the symmetry to C_{4v}. The out of plane distance of the zinc(II) atom is 28 (±6) pm and the associated Zn-N bond length 198.7 (±0.7) pm. A survey of known Zn-N bond distances in complexes with various coordination numbers and geometries reveals that observed Zn-N bond lengths are typically longer than 206 pm, even in their favoured tetrahedral configuration. A result which seems to disagree with the X-ray diffraction study by suggesting that the zinc(II) atom is too large to fit into the central hole of the phthalocyanine skeleton. Nevertheless, even in the gas phase the Zn-N bond length (198.7 (±0.7) pm) is, within one standard deviation, identical to the value found in the crystal (198.0 (±0.2) pm). Notably, the core of the macrocycle is somewhat expanded as compared to Fe(II) phthalocyanine to accommodate the relatively large Zn(II) atom [43].

Because the liquid phase is more closely related to the solid than to the gas phase, a symmetrized X-ray structure has been used for calculating the spectra of ZnPc making the rings perfectly planar and adopting D_{4h} symmetry. However, since C-H bond lengths are consistently too short (r_e = 95.0 pm) in X-ray structures, they have been adjusted to the value derived from the electron diffraction method (r_e = 108.0 pm).

Prediction of the spectroscopic features of zinc(II) phthalocyanine

Based on the chosen geometrical structure, the energy of the molecular ground state of ZnPc, $^1A_g(\pi)$, has been minimized in an iterative procedure using the closed-shell spin-restricted approach until self-consistency was achieved. The orbital eigenvalues of the highest occupied (HOMOs) and lowest unoccupied molecular orbitals (LUMOs) are given in figure 2. In agreement with recent CNDO/2 calculations [46], the HOMOs are of $a_{1u}(\pi)$ and $a_{2u}(\pi)$ symmetry in D_{4h} notation and the LUMOs are degenerate and of $e_g(\pi^*)$ symmetry. Notably, the energy gap between the $a_{1u}(\pi)$ and $a_{2u}(\pi)$ orbitals ($\Delta\varepsilon \approx 2.84$ eV) is significantly larger than the $a_{1u}(\pi)$–$a_{2u}(\pi)$ splitting found in zinc(II) porphyrin ($\Delta\varepsilon \approx 0.46$ eV; M Ochsner, preliminary calculations using the INDO/S model, 1995). A result which is in reasonable harmony with previous calculations using CNDO/2 [46] or extended Hückel approximations [47]. When the four bridging CH groups in the porphyrin ring system are replaced by N atoms, an increase of the energy gap between the $a_{1u}(\pi)$ and $a_{2u}(\pi)$ orbitals is well known and results mainly from inclusion of nitrogen lone pairs [48].

The ground state $A_{1g}(\pi)$ Mulliken population analysis of ZnPc is given in table I. As indicated, the zinc(II) atom has a net positive charge of 0.661 and slightly greater negative charges are found on the bridged compared to the central nitrogen atoms.

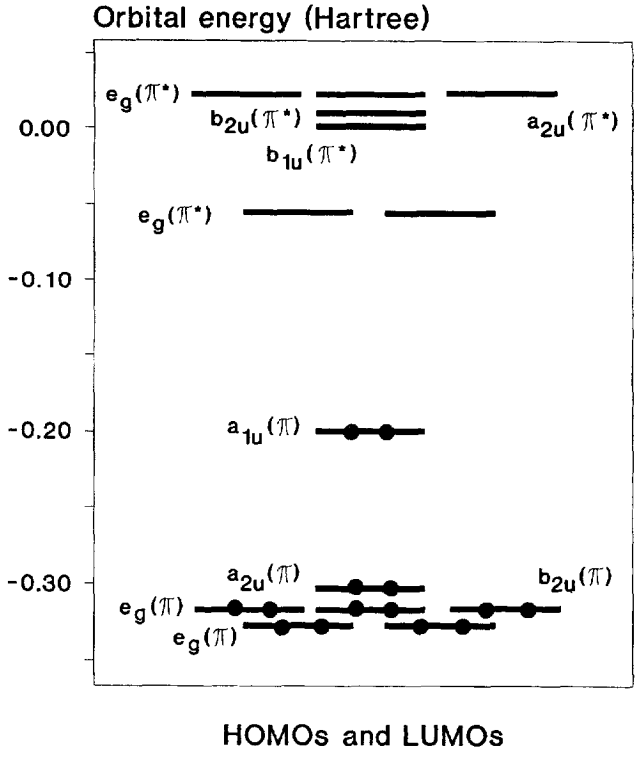

Fig 2. Window including the seven highest occupied (HOMOs) and lowest unoccupied SCF molecular orbitals (LUMOs) of zinc(II) phthalocyanine in its electronic ground state.

The excited state energies of ZnPc were obtained by setting up and diagonalizing CI matrices including single excitations only. Due to the high symmetry of the molecule under investigation (D_{4h}), C_{2v} and C_{2h} Abelian subgroup symmetries could be used to facilitate the CI calculation. After initial investigation with larger CI matrices, we found that transitions in the visible and UV region were adequately reproduced by including 440 single-substitution wavefunctions only (110 for each of the four irreducible representations in the C_{2v} symmetry group) for the calculation of excited configurations. Throughout the study the lowest 86 electrons of the reference configuration were frozen in the CI calculation.

As indicated in table II, the employed INDO/S model is capable of accurately predicting the most prominent singlet-singlet and triplet-triplet transitions found in the visible and UV region. The lowest allowed transitions were estimated with an accuracy of a few hundred wavenumbers as related to the experimentally observed bands.

The singlet-singlet absorption bands leading from the electronic ground state, $^1A_g(\pi)$, to the manifold of excited $^1E_u(\pi^*)$ states are labelled as **Q**, **B**, **N**, **L** and **C** in analogy to the nomenclature used for porphyrins [49]. However, while the S_1 state [$^1E_u^Q(\pi^*)$] almost purely consisted of $a_{1u}(\pi) \rightarrow e_g(\pi^*)$ configurations, all other $^1E_u(\pi^*)$ states were composed of a heterogeneous mixture of single-substitution determinants. In general $^1E_u(\pi^*)$ states possess a slightly distorted structure of symmetry D_{2h} as a result of host-field stabilized, Jahn–Teller effects (see below) and the corresponding $^1E_u(\pi^*) \leftarrow {}^1A_g(\pi)$ absorption bands are dipole allowed with a transition moment polarized in the molecular plane (x, y direction).

Table I. Electronic populations and net charges on the various atoms of ZnPc according to Mulliken.

Atom	*No*	*Electronic charge*	*Net charge*
Zn	–	1.339	0.661
N	1	5.400	–0.400
N	2	5.423	–0.423
C	3	3.702	0.298
C	4	3.994	0.006
C	5	4.044	–0.044
C	6	4.051	–0.051
H	7	0.934	0.066
H	8	0.946	0.054

The atoms are numbered as shown in figure 1.

The position of the $S_1 \leftarrow S_0$ (**Q**) absorption band (14 860 cm^{-1}) was slightly underestimated and predicted to be located at $\approx$ 14 310 cm^{-1} ($\approx$ 699 nm). Based on our calculations, the $S_1 \leftarrow S_0$ band predominantly (with contributions of $\approx$ 90%) arises from $a_{1u}(\pi) \rightarrow e_g(\pi^*)$ transitions with slight inclusions ($\approx$ 5%) of $a_{2u}(\pi) \rightarrow e_g(\pi^*)$ configurations. Notably, the first excited singlet state [$^1E_u^Q(\pi^*)$] consists of a degenerate pair of states as long as vibronic and/or environmental effects are neglected (fig 3a).

Taking interactions between electronic and vibrational angular momenta into account, the degenerate electronic wavefunctions of the S_1 state [$^1E_u^Q(\pi^*)$] are Jahn–Teller coupled to vibrational modes (b_{1g} and/or b_{2g}) which cause a non-symmetric displacement of the nuclei [50, 51]. The Jahn–Teller effect lowers the molecular symmetry from D_{4h} to D_{2h} by generating two identical potential surfaces ($|^1E_u^Q\, x\rangle$ and $|^1E_u^Q\, y\rangle$ of equal energy, but separated in the b_{1g}/b_{2g} configuration

Table II. Calculated versus observed transition frequencies and oscillator strengths of zinc(II) phthalocyanine.

Label	*Transition*	*Calculated (cm^{-1})*	f_{th}	*Observed*[a] *(cm^{-1})*	f_{exp}[a]	*Observed*[b] *(cm^{-1})*
Q	$^1E_u^Q(\pi^*) \leftarrow {}^1A_{1g}(\pi)$	14 310	1.65	14 860	1.70	15 130
B	$^1E_u^B(\pi^*) \leftarrow {}^1A_{1g}(\pi)$	31 510	1.05	29 110	1.00	30 630
N	$^1E_u^N(\pi^*) \leftarrow {}^1A_{1g}(\pi)$	34 700	0.75			36 230
L	$^1E_u^L(\pi^*) \leftarrow {}^1A_{1g}(\pi)$	41 470	0.30			41 670
C	$^1E_u^C(\pi^*) \leftarrow {}^1A_{1g}(\pi)$	45 720	0.55			45 460
	$^3E_u^Q(\pi^*) \leftarrow {}^1A_{1g}(\pi)$	9050	0.00	9070[c]	0.00	
	$^3A_{1g}(\pi^*) \leftarrow {}^3E_u^Q(\pi^*)$	19 790	0.75	20 410	0.50	

[a]Absorption maxima and oscillator strengths in $CHCl_3$ [1]. [b]Absorption maxima in the vapour phase [49]. [c]Value derived from the fluorescence quenching of zinc(II) phthalocyanine by the heavy atom solvent 1-iodopropane. Spectroscopically, the $T_1 \rightarrow S_0$ phosphorescence emission band was detected at 77 K in a frozen 2-methyltetrahydrofuran matrix and centered at around 9100 cm^{-1} [1].

space (fig 3b). The intersection point between the two Jahn–Teller surfaces occurs at ca 45 cm^{-1} in an argon matrix [51]. Environmental effects, ie, the force field of the host (V_{HF}), simultaneously shift the two potential energy wells by different amounts along the (vertical) energy scale thereby lifting their two-fold vibronic degeneracy, but without changing their shape (fig 3c) [52]. The energy splitting was measured to be 40 cm^{-1} in an argon [53] and 29 cm^{-1} in a Shpol'skii (α-chloronaphthalene/*n*-decane) matrix [54].

Subsequent to excitation of ZnPc to the S_1 state, Jahn–Teller distortions therefore reduce the molecular symmetry from D_{4h} to D_{2h}. Differences in the equilibrium geometries have been estimated using the non-spectroscopic INDO/1 version [25, 35] by minimizing the overall energy ($= E_{el} + E_{nuc}$) of the S_0 and S_1 state, respectively, in terms of internal coordinates. Based on a thorough group theoretical analysis the ZnPc molecule possesses 165 normal modes of vibrations including 41 double degenerate ones (28 e_u and 13 e_g in D_{4h} notation). Neglecting interactions with other vibronic states, the fundamental vibrations capable of coupling the $^1A_{1g}(\pi)$ with the $^1E_u^Q(\pi^*)$ state reduce to 55 active modes of symmetry: 14 a_{1g}, 13 a_{2g}, 14 b_{1g} and 14 b_{2g}. Since ZnPc contains at least 20, low frequency, vibrational modes ($\omega < 1000$ cm^{-1}) [53, 54] and differences exist between the geometries of the S_0 and S_1 states, higher Franck–Condon factors are expected to favour transitions from the vibronic ground state as well as from thermally excited vibrational levels of the S_0 state to a wide variety of vibrationally excited levels of the S_1 state. Subsequent to the excitation, the vibrational excess energy is rapidly ($\leq 10^{-11}$ s) dissipated and associated with a structural relaxation of the molecular frame ($D_{4h} \rightarrow D_{2h}$), leaving the fluorophore in the lowest vibrational level of the S_1 state prior to the radiative and non-radiative relaxation to the molecular ground state ($\tau_{S1} = 3.59(7)$ ns in ethanol [1]). Based on our calculations, the $S_1 \leftarrow S_0$ absorption band is postulated to be found in the range 660 to 720 nm and the associated emission band 690 to 760 nm.

Much to our astonishment, singlet-singlet transitions occurring in the near and far UV region were predicted with comparable accuracy as the $S_1 \leftarrow S_0$ absorption band (rms error $\approx$ 900 cm^{-1}). Nevertheless, the predictive power of the INDO/S model tends to be somewhat lower for transitions located in the UV region. The reason for this discrepancy is explained by the fact that only single excitations are taken into consideration for the construction of the CI matrix. The inclusion of higher-substitution wavefunctions particularly affects the positions of UV bands and the restriction to single excitations in general leads to an overestimation of the corresponding transition frequencies [30, 55].

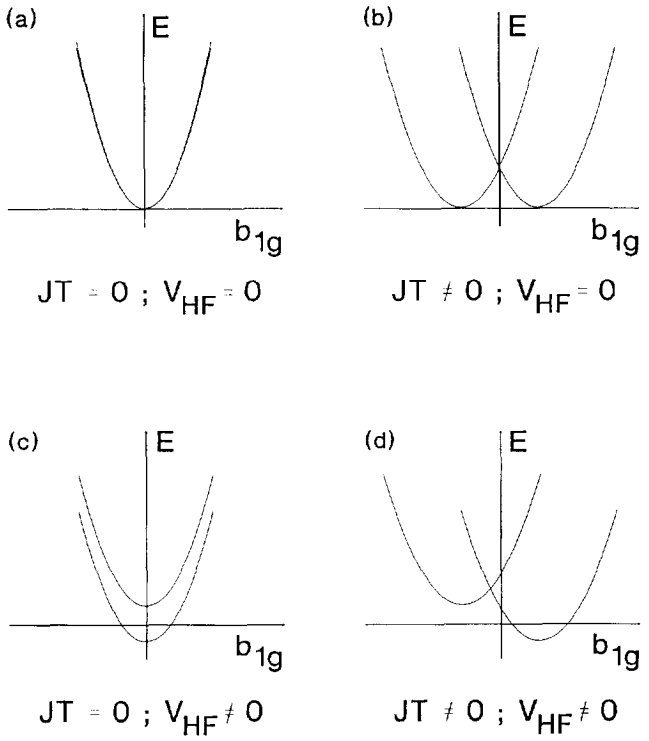

Fig 3. The potential surfaces ($|^1E_u^Q x\rangle$ and $|^1E_u^Q y\rangle$) representing the first excited singlet state of zinc(II) phthalocyanine in the presence and absence of Jahn–Teller (JT) and/or host-field effects (V_{HF}) [51–54].

The first excited triplet state T_1 was calculated to possess an excitation energy of 9050 cm^{-1} and the lowest allowed triplet-triplet transition ($T_n \leftarrow T_1$) was predicted to be located at around 19 790 cm^{-1} ($\approx$ 505 nm) with a polarization in the molecular plane. Based on these theoretical calculations, the $T_1 \leftarrow S_0$ phosphorescence emission could actually be observed at around 9100 cm^{-1} in a frozen 2-methyltetrahydofuran matrix [1]. In addition, the corresponding $T_n \leftarrow T_1$ absorption band was detected at around 490 nm in chloroform [1].

Compared to the porphyrins, the smaller ring size of the phthalocyanine skeleton gives rise to a larger ligand field. As postulated by Schaffer et al, the bridge nitrogen atoms should therefore enable $n \rightarrow \pi^*$ transitions which are expected to be located in the region of the Soret band [47]. Whereas such transitions have been theoretically predicted and spectroscopically assigned for the Fe(II) and Mn(II) complexes, the corresponding lines are missing in the spectra of phthalocyanines containing Mg(II) or Zn(II) as central atoms [46]. This result seems quite reasonable, since the Fe(II) and Mn(II) derivatives possess a strongly contracted phthalocyanine core compared to the

expanded Mg(II) or Zn(II) macrocycles [43, 56]. In agreement with these considerations, our calculation have not found $n \rightarrow \pi^*$ transitions for ZnPc in the range between 200 and 800 nm.

Despite the fact that the X-ray structure of ZnPc was quite different from the geometries obtained using Zerner's non-spectroscopic INDO/1 version [25, 35] or Stewart's MOPAC program [36], calculated spectra were identical within an rms error of around 200 cm^{-1}. This result seems to indicate that the transition frequencies tend to be rather insensitive to modest changes in the molecular geometry at least for phthalocyanine ring systems. In contrast, computed oscillator strengths were quite sensitive to small structural changes.

Comparison between theoretical and experimental oscillator strengths

Oscillator strengths have been estimated by calculating the matrix elements of the transition dipole moment operator ($e \cdot \mathbf{r}$) [57]:

$$f_{\text{theory}} = \frac{8 \cdot \pi^2 \cdot m_e \cdot c \cdot \omega_{mn}}{3 \cdot h \cdot e^2 \cdot d_m} \sum_{k,j} \left| \langle \Psi_{m_k} \left| \sum_{i=1}^{p+q} e \cdot \mathbf{r}_i \right| \Psi_{n_j} \rangle \right|^2$$

Here m_e and e give the mass and the charge of the electron, ω_{mn} (cm^{-1}) corresponds to the transition frequency and d_m refers to the degeneracy of the lower state with the summation taken over all combinations of sublevels m_k and n_j. In Zerner's program, the evaluation of the length of the transition dipole ($\mathbf{r}$) only includes one-center charge and polarization terms, but neglects two-center bond contributions [21].

Of course, if for a given transition the computed oscillator strength is zero, the corresponding spectral line may still appear in the absorption spectrum if the matrix elements of the magnetic dipole or electric quadrupole moment are different from zero.

As shown in table II, the theoretically predicted oscillator strengths are in excellent agreement with the experimental values [1], which have been calculated from the integral extinction coefficient of the corresponding absorption band [58]:

$$f_{\text{experimental}} = 4.319 \times 10^{-9} \int \varepsilon(\omega) \cdot d\omega; \quad \omega(\text{cm}^{-1})$$

The photosensitizing properties of ZnPc as derived from the INDO/S calculation

Based on the theoretically predicted properties, we conclude that ZnPc possesses an intensive absorption band at around 699 nm, ie, at a wavelength where the penetration depth of light is considerably larger than that of Photofrin ($\lambda \approx 630$ nm) [3]. Moreover, the excitation energy of the first excited triplet state is high enough to enable the generation of $^1\Delta_g O_2$. Owing to the small gap between the excitation energies of ^{3}ZnPc (9050 cm^{-1}) and of $^1\Delta_g O_2$ (7900 cm^{-1}) Franck–Condon factors are expected to strongly promote Type II reaction processes. Contrasting these results, the S_1–T_1 energy gap ($\Delta E_{th} \approx 5360$ cm^{-1}) is far too small to trigger the formation of singlet oxygen.

Consistent with the high oscillator strength, the lifetime of the first excited singlet state is too short to allow ample bimolecular collisions with substrate molecules [59], as a consequence of which electron transfer reactions (Type I mechanism) may only occur from the lowest lying triplet state. The tendency of ZnPc to promote electron transfer reactions (oxidations and/or reductions) therefore primarily depends on the redox potentials in its first excited triplet state. Based on preliminary quantum chemical calculations, reduction or oxidation of ZnPc leads to the formation of π-radical anions or cations of symmetry D_{2h} and D_{4h}, respectively, with charges delocalized on the phthalocyanine macrocycle (M Ochsner, unpublished results, 1995).

By neglecting changes in the entropy and interactions with solvent molecules, the redox potentials of ^{3}ZnPc can be calculated from the redox potentials of the sensitizer in its electronic ground state and from the excitation energy (E_T) of the first excited triplet state (table III; [60]):

$$E_0(^3\text{ZnPc}^*/^2\text{ZnPc}^-) = E_0(\text{ZnPc}/^2\text{ZnPc}^-) + E_T/F$$

$$E_0(^2\text{ZnPc}^+/^3\text{ZnPc}^*) = E_0(^2\text{ZnPc}^+/\text{ZnPc}) - E_T/F$$

where F corresponds to the Faraday constant (F = 8067 cm^{-1}/V).

Based on the results obtained, we conclude that the tendency of ZnPc, even in its first excited triplet state, to react via a Type I reaction mechanism is very unlikely. Type II reaction are therefore expected to dominate the processes which initiate the tumour necrosis.

Concluding remarks and limitations of the INDO/S model

Experimentally, the most rewarding approach to determine the excitation energy of the lowest lying triplet state has been to record the corresponding $T_1 \rightarrow S_0$ phosphorescence spectrum. Since such transitions are spin-forbidden by nature, they are very weak and difficult to detect even in a frozen matrix. It is therefore useful for the experimental scientist to possess a theoretical tool to estimate the position of the $T_1 \rightarrow S_0$ emission band. In order to predict the energy of

Table III. Redox potentials of zinc(II) phthalocyanine in the ground and first excited triplet state (V).

Reaction	*Redox potential (V)*
Ground state	
$E_0(ZnPc/^2ZnPc^-)$	−0.65 [1, 61]
$E_0(^2ZnPc^+/ZnPc)$	+0.92 [1, 61]
First excited triplet state	
$E_0(^3ZnPc^*/^2ZnPc^-)$	+0.47
$E_0(^2ZnPc^+/^3ZnPc^*)$	−0.20

the first excited triplet state and other distinct spectroscopic properties of molecules of the size of zinc(II) phthalocyanine, various semiempirical programs (Extended Hückel, CNDO, INDO, MINDO/3, MNDO, MOPAC and PPP) with numerous parameterizations have been tested. To our belief, the most reliable program has been introduced by Zerner and has therefore been extensively discussed in this paper. A simple modification of the time-honoured INDO method of Pople allows a prediction of the singlet and triplet state properties (transition frequencies and intensities) of molecules of the size of zinc(II) phthalocyanine with an rms error of less than 1000 cm^{-1}.

Due to the truncation of the CI matrices, the presented model cannot yet account for states that are principally double excitations by nature. This shortcoming limits the described approach to molecules which do not possess such transitions in the visible or near UV region.

Acknowledgments

Thanks are due to M Nonella with whom preliminary calculations using the INDO/S approach have been performed in 1990 at the Max-Planck-Institut für Biochemie in Martinsried (Germany). The author gratefully acknowledges financial support from the Schweizerische Krebsliga.

References

1 Ochsner-Bruderer M (1994) Zinc(II) phthalocyanine, a Photosensitizer for Photodynamic Therapy of Tumors. Inaugural Dissertation, University of Basle, Basle, Switzerland
2 van den Bergh H (1986) *Chem Br* 22, 430–439
3 Eichler J, Knof J, Lenz H (1977) *Rad Environm Biophys* 14, 239–242
4 Rosenthal I (1991) *Photochem Photobiol* 53, 859–870
5 Roberts WG, Smith KM, McCullough JL, Berns MW (1989) *Photochem Photobiol* 49, 431–438
6 Fisher AMR, Murphree AL, Gomer CJ (1995) *Lasers Surg Med* 17, 2–31
7 Schieweck K, Capraro HG, Isele U et al (1994) In: *Photodynamic Therapy of Cancer* (Jori G, Moan J, Star WM, eds), Budapest, Hungary, *Proc SPIE*, 2078, 107–118
8 Isele U, van Hoogevest P, Leuenberger H, Capraro HG, Schieweck K (1994) In: *Photodynamic Therapy of Cancer* (Jori G, Moan J, Star WM, eds), Budapest, Hungary, *Proc SPIE*, 2078, 397–403
9 Takemura T, Ohta N, Nakajima S, Sakata I (1989) *Photochem Photobiol* 50, 339–344
10 Rosenthal I, Ben-Hur E (1989) In: *Phthalocyanines. Properties and Applications* (Leznoff CC, Lever ABP, eds) VCH Publishers, New York, 393–425
11 Patterson MS, Wilson BC, Graff R (1990) *Photochem Photobiol* 51, 343–349
12 Iu KK, Ogilby PR (1987) *J Phys Chem* 91, 1611–1617
13 Schmidt R, Bodesheim M (1994) *J Phys Chem* 98, 2874–2876
14 Parr RG (1972) *The Quantum Theory of Molecular Electronic Structure*. Benjamin WA, Massachusetts
15 Pancír J, Matoušek I, Zahradník R (1973) *Collection Czechoslov Chem Commun* 38, 3039–3066
16 Pople JA, Segal GA (1966) *J Chem Phys* 44, 3289–3296
17 Pople JA, Beveridge DL (1970) *Approximate Molecular Orbital Theory*. McGraw Hill, New York
18 Del Bene J, Jaffé HH (1968) *J Chem Phys* 48, 1807–1813
19 Del Bene J, Jaffé HH (1968) *J Chem Phys* 48, 4050–4055
20 Pople JA, Beveridge DL, Dobosch PA (1967) *J Chem Phys* 47, 2026–2033
21 Ridley JE, Zerner MC (1973) *Theor Chim Acta* 32, 111–134
22 Ridley JE, Zerner MC (1976) *Theor Chim Acta* 42, 223–236
23 Roothaan CCJ (1951) *Rev Mod Phys* 23, 69–89
24 Hall GG (1951) *Proc R Soc (London) A* 205, 541–552
25 Bacon AD, Zerner MC (1979) *Theor Chim Acta* 53, 21–54
26 Anderson WP, Edwards WD, Zerner MC (1986) *Inorg Chem* 25, 2728–2732
27 Zerner MC, Loew GH, Kirchner RF, Mueller-Westerhoff UT (1980) *J Am Chem Soc* 102, 589–599
28 Edwards WD, Zerner MC (1987) *Theor Chim Acta* 72, 347–361
29 Slater JC (1930) *Phys Rev* 36, 57–64
30 Hehre WJ, Radom L, Schleyer PvR, Pople JA (1986) *Ab Initio Molecular Orbital Theory*. John Wiley & Sons, New York
31 Kotzian M, Rösch N, Zerner MC (1992) *Theor Chim Acta* 81, 201–222
32 Schulz J, Iffert R, Jug K (1985) *Int J Quantum Chem* 27, 461–464
33 Boyd DB, Lipkowitz KB (1982) *J Chem Educ* 59, 269–274
34 Allinger NL (1977) *J Am Chem Soc* 99, 8127–8134
35 Anderson WP, Cundari TR, Drago RS, Zerner MC (1990) *Inorg Chem* 29, 1–3
36 Stewart JJP (1990) *J Comput-Aided Mol Des* 4, 1–105
37 Head JD, Zerner MC (1986) *Chem Phys Lett* 131, 359–366
38 Herman ZS, Kirchner RF, Loew GH, Mueller-Westerhoff UT, Nazzal A, Zerner MC (1982) *Inorg Chem* 21, 46–56
39 Møller C, Plesset MS (1934) *Phys Rev* 46, 618–622
40 Mataga N, Nishimoto K (1957) *Z Physik Chem* 13, 140–157
41 Pariser R, Parr RG (1953) *J Chem Phys* 21, 767–776
42 Zollinger H (1976) *Chemische Grundlagen der Farbenchemie*. Juris Druck und Verlag, Zürich, Switzerland
43 Scheidt WR, Dow W (1977) *J Am Chem Soc* 99, 1101–1104
44 Mihill A, Buell W, Fink M (1993) *J Chem Phys* 99, 6416–6420
45 Burkert U, Allinger NL (1982) *Molecular Mechanics*. ACS Monograph 177, American Chemical Society, Washington, DC
46 Maslov VG (1980) *Teor Eksp Khim* 16, 93–97
47 Schaffer AM, Gouterman M, Davidson ER (1973) *Theor Chim Acta* 30, 9–30
48 Dvornikov SS, Knyukshto VN, Kuzmitsky VA, Shulga AM, Solovyov KN (1981) *J Lumin* 23, 373–392
49 Edwards L, Gouterman M (1970) *J Mol Spectrosc* 33, 292–310
50 Bersuker IB (1984) *The Jahn–Teller Effect and Vibronic Interactions in Modern Chemistry*. Plenum Press, New York
51 Metcalf DH, VanCott TC, Snyder SW, Schatz PN, Williamson BE (1990) *J Phys Chem* 94, 2828–2832
52 Canters GW (1981) *J Chem Phys* 74, 157–162
53 VanCott TC, Rose JL, Misener GC et al (1989) *J Phys Chem* 93, 2999–3011
54 Huang TH, Rieckhoff KE, Voigt EM (1982) *J Chem Phys* 77, 3424–3441
55 Edwards WD, Zerner MC (1985) *Can J Chem* 63, 1763–1772
56 Fischer MS, Templeton DH, Zalkin A, Calvin M (1971) *J Am Chem Soc* 93, 2622–2628
57 Herzberg G (1966) *Electronic Spectra and Electronic Structure of Polyatomic Molecules*. Van Nostrand Reinhold, New York, 417–419
58 Atkins PW (1982) *Physical Chemistry*. 2nd edition, Oxford University Press, Oxford, 606–607
59 Birks JB (1970) *Photophysics of Aromatic Molecules*. John Wiley & Sons, London, 87–89
60 Balzani V, Bolletta F, Gandolfi MT, Maestri M (1978) *Top Curr Chem* 75, 1–64
61 Lexa D, Reix M (1974) *J Chim Phys Physicochim Biol* 71, 511–513